Available online at www.sciencedirect.com

SCIENCE DIRECT®

Engineering Fracture Mechanics 73 (2006) 963–977

Engineering Fracture Mechanics

www.elsevier.com/locate/engfracmech

Modal analysis of multi-cracked beams with circular cross section

Murat Kisa [a,*], M. Arif Gurel [b]

[a] Department of Mechanical Engineering, Faculty of Engineering, Harran University, Sanliurfa, Turkey
[b] Department of Civil Engineering, Faculty of Engineering, Harran University, Sanliurfa, Turkey

Received 11 October 2005; received in revised form 29 December 2005; accepted 2 January 2006

Abstract

This paper proposes a numerical model that combines the finite element and component mode synthesis methods for the modal analysis of beams with circular cross section and containing multiple non-propagating open cracks. The model virtually divides a beam into a number of parts from the crack sections and couples them by flexibility matrices considering the interaction forces that are derived from the fracture mechanics theory. The main feature of the presented approach is that the natural frequencies and mode shapes of a beam with an arbitrary number of cracks and any kind of two end conditions can be conveniently determined with a reasonable computational time. Three numerical examples are given to investigate the effects of location and depth of cracks on the natural frequencies and mode shapes of the beams. Moreover, it is shown through these examples that the evaluation of modal data obtained by the proposed model gives valuable information about the location and size of defects in the beams.

Keywords: Vibration; Multicracks; Finite element analysis; Vibration based detection of cracks

1. Introduction

Mechanical vibrations, long-term service or applied cyclic loads may result in the initiation of structural defects such as cracks in the structures. Accordingly, the determination of the effects of these deficiencies on the vibration safety and stability of the structures is an important task of engineers. Cracks in a structural element modify its stiffness and damping properties. In view of that, the modal data of the structure hold information relating to the place and dimension of the defect. Vibration analysis allowing online inspection is a novel and attractive method to detect cracks in the structures. The effects of the cracks on the dynamical behaviour of the structures have been the subject of many researchers in the past (Cawley and Adams [1], Gounaris and Dimarogonas [2], Shen and Chu [3], Krawczuk and Ostachowicz [4], Ruotolo et al. [5], Kisa et al. [6], Shifrin and Ruotolo [7], Kisa and Brandon [8,9], Viola et al. [10], Krawczuk [11], Patil and Maiti

* Corresponding author. Tel.: +90 533 4524865; fax: +90 414 3440031.
E-mail address: mkisa@harran.edu.tr (M. Kisa).

0013-7944/$ - see front matter
doi:10.1016/j.engfracmech.2006.01.002

Nomenclature

a	crack depth
A	crack area
u, v	displacements with respect to x and y axes
θ	rotation about z axis
m	number of components
L	length of the beam
D	diameter of the beam
R	radius of the beam
R/L	slenderness ratio
a/D	crack depth ratio
L_i/L	crack position
E	Young's modulus of elasticity
v	Poisson's ratio
ρ	material density
K_{I}	stress intensity factor for mode I
K_{II}	stress intensity factor for mode II
K_{III}	stress intensity factor for mode III
J	strain energy release rate
U	strain energy
c_{ij}	flexibility coefficients
C	flexibility matrix
K_i	stiffness matrix for element i
M_i	mass matrix for element i
K_{cr}	stiffness matrix induced by the crack
K_{C}	connection matrix
F	exerted force of a spring
P_i	applied loads
u_i	additional displacement caused by the crack
$\mathbf{q}$	generalised displacement vector
$\mathbf{f}(t)$	external force vector
$\mathbf{g}(t)$	applied force vector
$\mathbf{d}(t)$	spring force vector
$\mathbf{s}$	principal coordinate vector
ω	natural frequency
ω_{cr}	natural frequency of the cracked beam
ω_{nc}	natural frequency of the non-cracked beam
ϕ_{ij}	modal matrix
ψ_{ij}	mass normalised modal matrix

[12], Kisa [13]). Gudmundson [14] investigated the influence of small cracks on the natural frequencies of slender structures by perturbation method as well as by transfer matrix approach. Yuen [15] proposed a methodical finite element procedure to establish the relationship between damage location, damage size and the corresponding modification in the eigenparameters of a cantilever beam. Qian et al. [16] developed a finite element model of an edge-cracked beam. Rizos et al. [17] denoted the crack as a massless rotational spring, whose stiffness was computed by making use of the fracture mechanics. Shen and Taylor [18] presented a detection process to reveal the crack characteristics from vibration measurements.

Most studies on the vibration analysis of circular beams and shafts deal with single crack. Dimarogonas and Papadopoulos [19], by using the theory of cracked shafts with dissimilar moments of inertia, investigated the vibration of cracked shafts in bending. Papadopoulos and Dimarogonas [20] studied the free vibration of shafts and presented the influence of the crack on the vibration behaviour of the shafts. Kikidis and Papadopoulos [21] analysed the influence of the slenderness ratio of a non-rotating cracked shaft on the dynamic characteristics of the structure. Zheng and Fan [22] studied the vibration and stability of cracked hollow-sectional beams. Dong et al. [23] presented a continuous model for vibration analysis and parameter identification of a non-rotating cracked rotor. They assumed that the cracked rotor was an Euler–Bernoulli beam with circular cross section. The occurrence of multiple cracks has been studied by a few researchers. Tsai and Wang [24], Darpe et al. [25] and Sekhar [26,27] analysed the vibration of multi-crack rotors. Ruotolo and Surace [28] presented the damage assessment of multiple cracked beams by using the modal parameters of the lower modes. Zheng and Fan [29] analysed free vibration of a non-uniform beam with multiple cracks by using a kind of modified Fourier series. Li [30,31] offered an analytical formulation using boundary conditions and recursive formulas by which he analysed the free vibration of beams with an arbitrary number of cracks and concentrated masses. Khiem and Lien [32] and Lin et al. [33] used the transfer matrix method for the natural frequency analysis of beams with an arbitrary number of cracks. Ruotolo and Surace [34] proposed the smooth function method to calculate the natural frequencies of a vibrating isotropic bar with multiple cracks. Patil and Maiti [35] experimentally verified a method for prediction of location and size of multiple cracks based on measurement of natural frequencies of slender multi-cracked cantilever beams. Chang and Chen [36] presented a technique for the detection of the location and size of cracks in the multiple cracked beams by spatial wavelet based approach. Recently, Binici [37] investigated the vibration of beams with multiple open cracks subjected to axial force. His method uses one set of end conditions as initial parameters for determining the mode shape functions.

Abraham and Brandon [38] and Brandon and Abraham [39] presented a method utilising substructure normal modes to predict the vibration properties of a cantilever beam with a closing crack. The full eigensolution of a structure containing substructures each having large number of degrees of freedom can be costly in computing time. A method known as component mode synthesis or substructure technique, proposed by Hurty [40], enabled the problem to be broken up into separate elements and thus considerably reduced its complexity. The component mode synthesis method was initially developed to ease the study of very large structures but in this study it is used for another purpose. The advantage of the method in the case of a non-linear cracked beam stems from the fact that, when a beam is split into components from the crack sections, each substructure becomes linear and analytical or numerical results are available for their normal modes. Consequently, the initial non-linear system with local discontinuities in stiffness at the crack sections is now composed of a number of linear segments. An important characteristic of the model developed in this study is that it allows discontinuity in the displacement field at the crack sections when the crack is open. Substructures are connected by artificial and massless springs whose stiffness coefficients are functions of the flexibility coefficients. To the best of the authors' knowledge, the presented method is applied for the first time to the multi-cracked beams of circular cross section which commonly used in engineering structures.

2. Theoretical model

The model chosen is a cantilever beam of length L and diameter D ($D = 2R$), having transverse open edge cracks of depth a_i at variable positions L_i (Fig. 1). The beam has $m - 1$ cracks; therefore it is divided into m components from the crack sections leading to a substructure approach. Accordingly, as aforementioned, the global non-linear system with local stiffness discontinuities is detached into m linear subsystems. Every part is also broken up into finite elements with two nodes and three degrees of freedom at the each node as shown in Fig. 2.

2.1. Evaluation of local flexibility matrix of a cracked beam with circular cross section

As a result of the strain energy concentration at the neighbouring area of the crack tip, the existence of cracks in structures is a resource of local flexibility which consequently influences the dynamic properties of the structures. In the linear elastic range, these flexibility coefficients are expressed by stress intensity factors

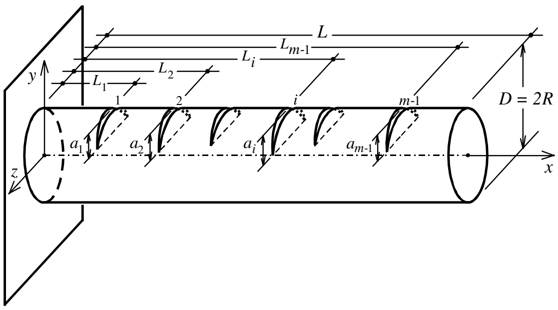

Fig. 1. Geometry of a multi-cracked beam with circular cross section.

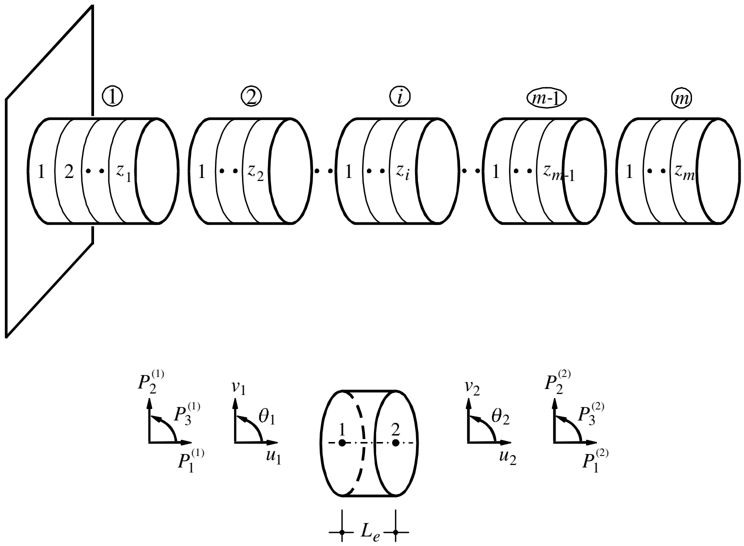

Fig. 2. Finite element model of the multi-cracked circular beam.

derived through Castigliano's theorem. The strain energy release rate, J, represents the elastic energy in relation to a unit increase in length ahead of the crack front. For plane strain, J can be given as (Irwin [41])

$$J = \frac{1-v^2}{E}K_{\mathrm{I}}^2 + \frac{1-v^2}{E}K_{\mathrm{II}}^2 + \frac{1+v}{E}K_{\mathrm{III}}^2 \tag{1}$$

where v, E, K_{I}, K_{II} and K_{III} are Poisson's ratio, modulus of elasticity and the stress intensity factors for the mode I, II and III deformation types, respectively. As torsional effects will not be concerned about in this study, simply mode I and mode II types of deformations are considered. If U is the strain energy of a cracked structure with a crack area A under the load P_i, then the relation between J and U is

$$J = \frac{\partial U(P_i, A)}{\partial A} \tag{2}$$

Consistent with the Castigliano's theorem, the additional displacement caused by the crack in the direction of P_i can be given as

$$u_i = \frac{\partial U(P_i, A)}{\partial P_i} \tag{3}$$

Substituting Eq. (2) into Eq. (3) gives the final expression between displacement and strain energy release rate J as

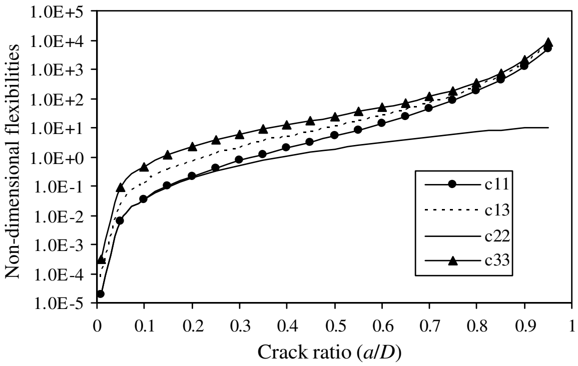

Fig. 3. Non-dimensional compliance coefficients as a function of the crack depth ratio a/D.

$$u_i = \frac{\partial}{\partial P_i} \int_A J(P_i, A)\mathrm{d}A \tag{4}$$

Now the flexibility coefficients which are the functions of the crack shape and the stress intensity factors can be introduced as follows:

$$c_{ij} = \frac{\partial u_i}{\partial P_j} = \frac{\partial^2}{\partial P_i \partial P_j} \int_A J(P_i, A)\mathrm{d}A \tag{5}$$

The flexibility coefficients c_{ij} are obtained from the fracture mechanics method proposed by Dimarogonas and Paipetis [42]. Dimensionless flexibility coefficients are calculated numerically and drawn in Fig. 3. Since the shear force does not contribute to the opening mode of the crack, the flexibility matrix, in relation to displacement vector $\delta(u, v, \theta)$, can be written as

$$C = \begin{bmatrix} c_{11} & 0 & c_{13} \\ 0 & c_{22} & 0 \\ c_{31} & 0 & c_{33} \end{bmatrix}_{(3\times 3)} \tag{6}$$

Using the flexibility matrix, the stiffness matrix induced by a crack is given as

$$K_{\mathrm{cr}} = \begin{bmatrix} C^{-1} & -C^{-1} \\ -C^{-1} & C^{-1} \end{bmatrix}_{(6\times 6)} \tag{7}$$

In the literature, there are flexibility coefficient equations relating to the other cross sections. For instance, regarding a rectangular cross section one can find the flexibility coefficients in the study of Kisa and Brandon [8].

2.2. Coupling of the substructures by springs

Consider all components ($i = 1, 2, \ldots, m$) which are undamped and connected to each other by means of springs capable of carrying axial, shearing and bending effects, Fig. 4. The stiffness of each spring is determined from Eq. 7. For an uncracked beam with m elements the equation of motion, in matrix notation, is given as

$$\begin{bmatrix} M_1 & 0 & \ldots & 0 \\ 0 & M_2 & \ldots & 0 \\ \ldots & \ldots & \ldots & \ldots \\ 0 & 0 & 0 & M_m \end{bmatrix} \begin{Bmatrix} \ddot{q}_1 \\ \ddot{q}_2 \\ \ldots \\ \ddot{q}_m \end{Bmatrix} + \begin{bmatrix} K_1 & 0 & \ldots & 0 \\ 0 & K_2 & \ldots & 0 \\ \ldots & \ldots & \ldots & \ldots \\ 0 & 0 & 0 & K_m \end{bmatrix} \begin{Bmatrix} q_1 \\ q_2 \\ \ldots \\ q_m \end{Bmatrix} = \begin{Bmatrix} f_1(t) \\ f_2(t) \\ \ldots \\ f_m(t) \end{Bmatrix} \tag{8}$$

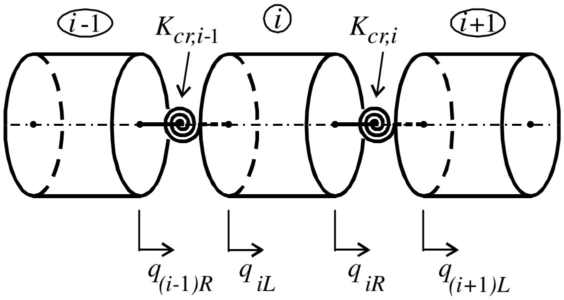

Fig. 4. Coupling the components by springs.

where $\mathbf{q}$ and $\mathbf{f}(t)$ are the generalised displacement and external force vector, respectively. M_i and K_i, $i = 1, \ldots, m$, are mass and stiffness matrices for the elements, respectively. Mass and stiffness matrices are taken from the paper of Friedman and Kosmatka [43]. Eq. (8) gives the eigenvalue equation as

$$\left(\begin{bmatrix} K_1 & 0 & \ldots & 0 \\ 0 & K_2 & \ldots & 0 \\ \ldots & \ldots & \ldots & \ldots \\ 0 & 0 & 0 & K_m \end{bmatrix} - \begin{bmatrix} \omega_1^2 & 0 & \ldots & 0 \\ 0 & \omega_2^2 & \ldots & 0 \\ \ldots & \ldots & \ldots & \ldots \\ 0 & 0 & 0 & \omega_m^2 \end{bmatrix}\begin{bmatrix} M_1 & 0 & \ldots & 0 \\ 0 & M_2 & \ldots & 0 \\ \ldots & \ldots & \ldots & \ldots \\ 0 & 0 & 0 & M_m \end{bmatrix}\right)\begin{Bmatrix} q_1 \\ q_2 \\ \ldots \\ q_m \end{Bmatrix} = \begin{Bmatrix} 0 \\ 0 \\ \ldots \\ 0 \end{Bmatrix} \tag{9}$$

By utilising Eq. (9) natural frequencies and mode shapes of each component can be obtained.

On particular springs, the exerted forces F_1, $F_{2\mathrm{L}}$,$F_{2\mathrm{R}}$,$F_{3\mathrm{L}}, \ldots, F_{(m-1)\mathrm{R}}$ and F_m, can be given as

$$\begin{aligned} &F_1 = K_{\mathrm{cr},1}(q_1 - q_{2\mathrm{L}}) \\ &F_{2\mathrm{L}} = K_{\mathrm{cr},1}(q_{2\mathrm{L}} - q_1) \\ &F_1 = -F_{2\mathrm{L}} \\ &F_{2\mathrm{R}} = K_{\mathrm{cr},2}(q_{2\mathrm{R}} - q_{3\mathrm{L}}) \\ &F_{3\mathrm{L}} = K_{\mathrm{cr},2}(q_{3\mathrm{L}} - q_{2\mathrm{R}}) \\ &F_{2\mathrm{R}} = -F_{3\mathrm{L}} \\ &\ldots \\ &F_{(m-1)\mathrm{R}} = K_{\mathrm{cr},m-1}(q_{(m-1)\mathrm{R}} - q_m) \\ &F_m = K_{\mathrm{cr},m-1}(q_m - q_{(m-1)\mathrm{R}}) \\ &F_{(m-1)\mathrm{R}} = -F_m \end{aligned} \tag{10}$$

where $q_1, q_{2\mathrm{L}}, q_{2\mathrm{R}}, q_{3\mathrm{L}}, \ldots, q_{(m-1)\mathrm{R}}$ and q_m are the displacements of the connection points and $K_{\mathrm{cr},i}$, $i = 1, \ldots, m-1$, are the stiffness matrices due to cracks and developed by Eq. (7). Here L and R stand for the left and right ends of a component, respectively. Eq. (10) can be written as

$$\begin{Bmatrix} F_1 \\ F_{2\mathrm{L}} \\ F_{2\mathrm{R}} \\ F_{3\mathrm{L}} \\ \ldots \\ F_{(m-1)\mathrm{R}} \\ F_m \end{Bmatrix} = [K_\mathrm{C}]\begin{Bmatrix} q_1 \\ q_{2\mathrm{L}} \\ q_{2\mathrm{R}} \\ q_{3\mathrm{L}} \\ \ldots \\ q_{(m-1)\mathrm{R}} \\ q_m \end{Bmatrix} \tag{11}$$

where K_C is the connection matrix and given as

$$K_C = \begin{bmatrix} K_{cr,1} & 0 & \dots & 0 \\ 0 & K_{cr,2} & \dots & 0 \\ \dots & \dots & \dots & \dots \\ 0 & 0 & \dots & K_{cr,m-1} \end{bmatrix} \tag{12}$$

The force vector $\mathbf{f}(t)$ comprises applied forces $\mathbf{g}(t)$ and forces resulting from the springs $\mathbf{d}(t)$, such that

$$\mathbf{f}(t) = \mathbf{g}(t) + \mathbf{d}(t) \tag{13}$$

From the equilibrium

$$\mathbf{d}(t) = -[K_C]\begin{Bmatrix} q_1 \\ q_{2L} \\ q_{2R} \\ q_{3L} \\ \dots \\ q_{(m-1)R} \\ q_m \end{Bmatrix} \tag{14}$$

Assume that $\begin{Bmatrix} F_{iL} \\ F_{iR} \end{Bmatrix}$ and $\begin{Bmatrix} q_{iL} \\ q_{iR} \end{Bmatrix}$ are denoted as $\begin{Bmatrix} F_{iL} \\ F_{iR} \end{Bmatrix} = \{F_i\}$, $\begin{Bmatrix} q_{iL} \\ q_{iR} \end{Bmatrix} = \{q_i\}$, $i = 2, \dots, m-1$. Substituting Eqs. (13) and (14) into Eq. (8) gives

$$\begin{bmatrix} M_1 & 0 & \dots & 0 \\ 0 & M_2 & \dots & 0 \\ \dots & \dots & \dots & \dots \\ 0 & 0 & 0 & M_m \end{bmatrix}\begin{Bmatrix} \ddot{q}_1 \\ \ddot{q}_2 \\ \dots \\ \ddot{q}_m \end{Bmatrix} + \begin{bmatrix} K_1 & 0 & \dots & 0 \\ 0 & K_2 & \dots & 0 \\ \dots & \dots & \dots & \dots \\ 0 & 0 & 0 & K_m \end{bmatrix}\begin{Bmatrix} q_1 \\ q_2 \\ \dots \\ q_m \end{Bmatrix} = -[K_C]\begin{Bmatrix} q_1 \\ q_2 \\ \dots \\ q_m \end{Bmatrix} + \begin{Bmatrix} g_1(t) \\ g_2(t) \\ \dots \\ g_m(t) \end{Bmatrix} \tag{15}$$

or

$$\begin{bmatrix} M_1 & 0 & \dots & 0 \\ 0 & M_2 & \dots & 0 \\ \dots & \dots & \dots & \dots \\ 0 & 0 & 0 & M_m \end{bmatrix}\begin{Bmatrix} \ddot{q}_1 \\ \ddot{q}_2 \\ \dots \\ \ddot{q}_m \end{Bmatrix} + \left(\begin{bmatrix} K_1 & 0 & \dots & 0 \\ 0 & K_2 & \dots & 0 \\ \dots & \dots & \dots & \dots \\ 0 & 0 & 0 & K_m \end{bmatrix} + [K_C]\right)\begin{Bmatrix} q_1 \\ q_2 \\ \dots \\ q_m \end{Bmatrix} = \begin{Bmatrix} g_1(t) \\ g_2(t) \\ \dots \\ g_m(t) \end{Bmatrix} \tag{16}$$

If modal matrix ϕ_{ij} is normalised by the mass, the following expression is given

$$\psi_{ij} = \frac{\phi_{ij}}{\sqrt{m_{jj}}} \tag{17}$$

where ψ_{ij} is mass normalised modal matrix. Following transformation is used

$$\begin{Bmatrix} q_1 \\ q_2 \\ \dots \\ q_m \end{Bmatrix} = \begin{bmatrix} \Psi_1 & 0 & \dots & 0 \\ 0 & \Psi_2 & \dots & 0 \\ \dots & \dots & \dots & \dots \\ 0 & 0 & \dots & \Psi_m \end{bmatrix}\begin{Bmatrix} s_1 \\ s_2 \\ \dots \\ s_m \end{Bmatrix} \tag{18}$$

where $\mathbf{s}_i$, $i = 1, \dots, m$, are the principal coordinate vectors. By premultiplying ψ^T and substituting Eqs. (17) and (18) into Eq. (16), gives

$$\begin{bmatrix} I & 0 & \dots & 0 \\ 0 & I & \dots & 0 \\ \dots & \dots & \dots & \dots \\ 0 & 0 & \dots & I \end{bmatrix} \begin{Bmatrix} \ddot{s}_1 \\ \ddot{s}_2 \\ \dots \\ \ddot{s}_m \end{Bmatrix} + \begin{bmatrix} \omega_1^2 & 0 & \dots & 0 \\ 0 & \omega_2^2 & \dots & 0 \\ \dots & \dots & \dots & \dots \\ 0 & 0 & \dots & \omega_m^2 \end{bmatrix} \begin{Bmatrix} s_1 \\ s_2 \\ \dots \\ s_m \end{Bmatrix}$$
$$+ \begin{bmatrix} \Psi_1 & 0 & \dots & 0 \\ 0 & \Psi_2 & \dots & 0 \\ \dots & \dots & \dots & \dots \\ 0 & 0 & \dots & \Psi_m \end{bmatrix}^{\mathrm{T}} [K_{\mathrm{C}}] \begin{bmatrix} \Psi_1 & 0 & \dots & 0 \\ 0 & \Psi_2 & \dots & 0 \\ \dots & \dots & \dots & \dots \\ 0 & 0 & \dots & \Psi_m \end{bmatrix} \begin{Bmatrix} s_1 \\ s_2 \\ \dots \\ s_m \end{Bmatrix} = \begin{bmatrix} \Psi_1 & 0 & \dots & 0 \\ 0 & \Psi_2 & \dots & 0 \\ \dots & \dots & \dots & \dots \\ 0 & 0 & \dots & \Psi_m \end{bmatrix}^{\mathrm{T}} \begin{Bmatrix} g_1(t) \\ g_2(t) \\ \dots \\ g_m(t) \end{Bmatrix} \tag{19}$$

where

$$\begin{aligned} & I = \psi_1^{\mathrm{T}} M_1 \psi_1 = \psi_2^{\mathrm{T}} M_2 \psi_2 = \cdots = \psi_m^{\mathrm{T}} M_m \psi_m \\ & \omega_1^2 = \psi_1^{\mathrm{T}} K_1 \psi_1 \\ & \omega_2^2 = \psi_2^{\mathrm{T}} K_2 \psi_2 \\ & \dots \\ & \omega_m^2 = \psi_m^{\mathrm{T}} K_m \psi_m \end{aligned} \tag{20}$$

Eq. (19), for free vibration, gives the eigenvalue equation as

$$\left(\begin{bmatrix} \omega_1^2 & 0 & \dots & 0 \\ 0 & \omega_2^2 & \dots & 0 \\ \dots & \dots & \dots & \dots \\ 0 & 0 & \dots & \omega_m^2 \end{bmatrix} + \begin{bmatrix} \Psi_1 & 0 & \dots & 0 \\ 0 & \Psi_2 & \dots & 0 \\ \dots & \dots & \dots & \dots \\ 0 & 0 & \dots & \Psi_m \end{bmatrix}^{\mathrm{T}} [K_{\mathrm{C}}] \begin{bmatrix} \Psi_1 & 0 & \dots & 0 \\ 0 & \Psi_2 & \dots & 0 \\ \dots & \dots & \dots & \dots \\ 0 & 0 & \dots & \Psi_m \end{bmatrix} - \omega^2 \begin{bmatrix} I & 0 & \dots & 0 \\ 0 & I & \dots & 0 \\ \dots & \dots & \dots & \dots \\ 0 & 0 & \dots & I \end{bmatrix} \right) \begin{Bmatrix} s_1 \\ s_2 \\ \dots \\ s_m \end{Bmatrix} = \begin{Bmatrix} 0 \\ 0 \\ \dots \\ 0 \end{Bmatrix} \tag{21}$$

From Eq. (21) the natural frequencies and mode shapes of the system can be determined. After solving this equation, the displacements for each component are calculated by using Eq. (18). It is obvious that when there is no crack in the beam, the elements of K_{C} in Eq. (21) become zero.

3. Numerical examples and discussion

3.1. Cantilever beam with a crack

Most studies on the vibration analysis of circular cross sectional beams and shafts deal with single crack. In the literature, there are some studies on the vibration of multi-cracked circular beams such as the studies of Darpe et al. [25] and Sekhar [26,27]. Different from the current investigation, in these studies the circular beam was assumed to be rotating, for that reason to validate the presented method a single crack cantilever beam with circular cross section is considered. The geometrical properties of the beam are chosen as; length $L = 2$ m, slenderness ratio $R/L = 0.1$, 0.06 and 0.04. Calculation has been performed with the numerical values; Young's modulus $E = 216 \times 10^9$ N m^{-2}, Poisson's ratio $\nu = 0.33$ and material density $\rho = 7.85 \times 10^3$ kg m^{-3}.

Fig. 5 illustrates the first non-dimensional frequencies of the cracked beam as a function of the crack depth ratio (a/D) for several slenderness ratios R/L (0.1, 0.06, and 0.04). In the analysis the crack location is $L_1/L = 0.2$. First non-dimensional natural frequencies are normalised according to next equation

$$\omega = \omega_{\mathrm{cr}}/\omega_{\mathrm{nc}} \tag{22}$$

where ω_{cr} and ω_{nc} refer to the natural frequency of the cracked and non-cracked cantilever beams, respectively.

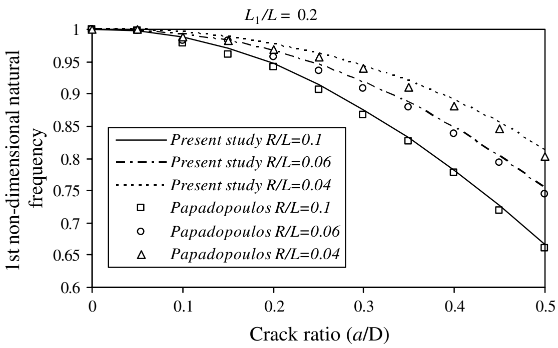

Fig. 5. First non-dimensional natural frequencies as a function of crack depth ratio, for several slenderness ratios $R/L = 0.1$, 0.06, 0.04 and crack position $L_1/L = 0.2$.

The natural frequencies of the cracked beam are lower than those of corresponding intact beam, as expected. Differences in the frequencies get higher as the depth of the crack increases. Because of the bending moment along the beam, which is concentrated at the fixed end, a crack closer to the free end will have a smaller effect on the fundamental frequency than a crack closer to the fixed end. It can be obviously seen from the Fig. 5 that when the slenderness ratio (R/L) increases, the frequency reduction gets higher, too. The results obtained by the current approach are compared with those of Papadopoulos and Dimarogonas [44] and the maximum differences between the results for the slenderness ratios (R/L) 0.1, 0.06 and 0.04 are calculated as 1.83%, 1.61% and 1.23%, respectively. As it is noticed from the Fig. 5, an excellent concurrence has been found between the results.

3.2. Cantilever beam with multiple cracks

Second example is chosen as a cantilever beam with three cracks. In the analysis, it is assumed that all cracks are at the same depth. The material and geometrical properties of the beam are identical to those of former case. For the present and subsequent examples, the slenderness ratio is taken as $R/L = 0.04$. Fig. 6 presents the first, second and third non-dimensional natural frequencies as a function of crack depth ratio for several crack locations ($L_1/L = 0.1$, $L_2/L = 0.2$, $L_3/L = 0.3$), ($L_1/L = 0.1$, $L_2/L = 0.5$, $L_3/L = 0.9$), ($L_1/L = 0.4$, $L_2/L = 0.5$, $L_3/L = 0.6$) and ($L_1/L = 0.7$, $L_2/L = 0.8$, $L_3/L = 0.9$). Non-dimensional natural frequencies are normalised according to Eq. (22). It is evident from the figure that the first frequency reduction is higher when the cracks are located near the fixed end ($L_1/L = 0.1$, $L_2/L = 0.2$, $L_3/L = 0.3$), while the frequency differences are higher in the second and third natural frequencies when the cracks are located near the midpoint ($L_1/L = 0.4$, $L_2/L = 0.5$, $L_3/L = 0.6$) and around 3/4 of the beam length ($L_1/L = 0.7$, $L_2/L = 0.8$, $L_3/L = 0.9$), respectively. When the cracks are located near the free end, the first natural frequency is almost unaffected even if the crack depth ratio is relatively high. The second and third natural frequencies are less affected when the cracks are near the fixed end and at the positions of ($L_1/L = 0.1$, $L_2/L = 0.5$, $L_3/L = 0.9$), respectively (see Fig. 6). As stated in the previous example, the changes in the natural frequencies get higher as the depth of the cracks increases.

Figs. 7–9 show the first, second and third natural bending mode shapes as a function of various crack depth ratios ($a/D = 0.2$, $a/D = 0.4$, $a/D = 0.6$) for several crack locations ($L_1/L = 0.1$, $L_2/L = 0.2$, $L_3/L = 0.3$), ($L_1/L = 0.1$, $L_2/L = 0.5$, $L_3/L = 0.9$), ($L_1/L = 0.4$, $L_2/L = 0.5$, $L_3/L = 0.6$) and ($L_1/L = 0.7$, $L_2/L = 0.8$, $L_3/L = 0.9$). From the mode shapes the position of the cracks can be clearly discerned. In some cases, from the mode shapes the crack detection may be very difficult and for these circumstances the natural frequencies can give useful information about the crack location. For instance, the first natural frequency changes are more useful than the first mode shapes when the cracks are located near the fixed end (see Figs. 6 and 7). As a consequence, in an inspection both natural frequencies and mode shapes should be considered.

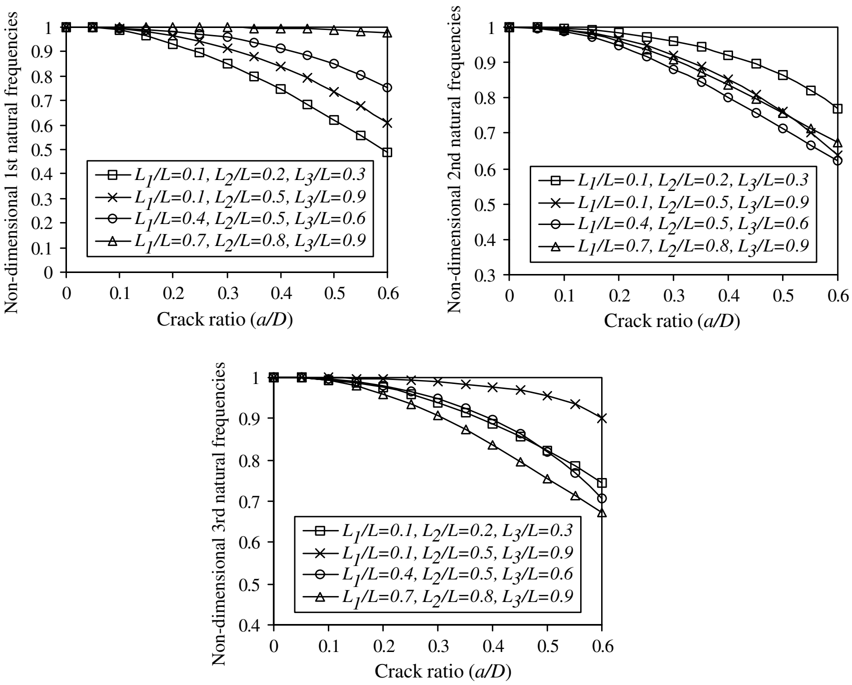

Fig. 6. First, second and third non-dimensional natural frequencies as a function of crack depth ratio for several crack locations ($L_1/L = 0.1$, $L_2/L = 0.2$, $L_3/L = 0.3$), ($L_1/L = 0.1$, $L_2/L = 0.5$, $L_3/L = 0.9$), ($L_1/L = 0.4$, $L_2/L = 0.5$, $L_3/L = 0.6$) and ($L_1/L = 0.7$, $L_2/L = 0.8$, $L_3/L = 0.9$).

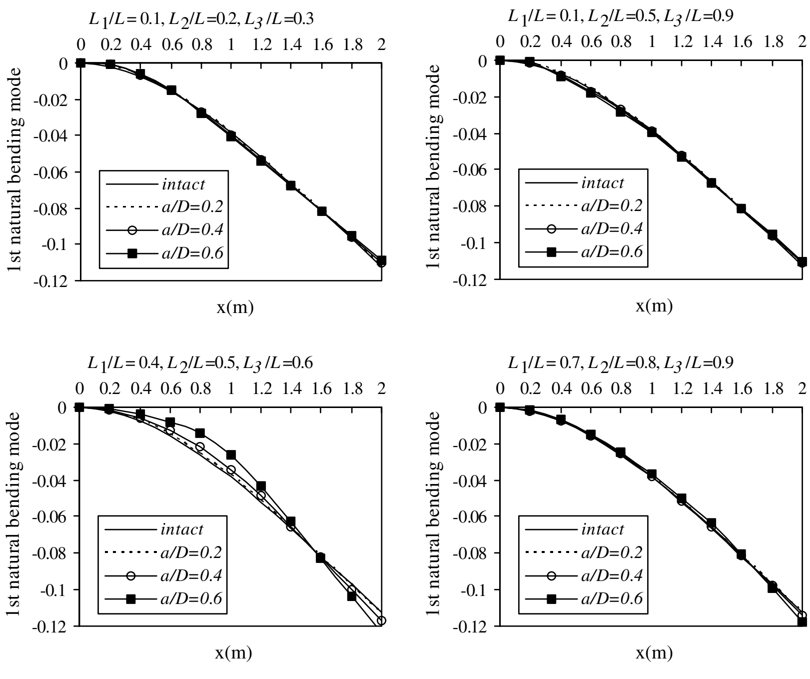

Fig. 7. First natural bending mode as a function of various crack depth ratios ($a/D = 0.2$, $a/D = 0.4$, $a/D = 0.6$) for several crack locations ($L_1/L = 0.1$, $L_2/L = 0.2$, $L_3/L = 0.3$), ($L_1/L = 0.1$, $L_2/L = 0.5$, $L_3/L = 0.9$), ($L_1/L = 0.4$, $L_2/L = 0.5$, $L_3/L = 0.6$) and ($L_1/L = 0.7$, $L_2/L = 0.8$, $L_3/L = 0.9$).

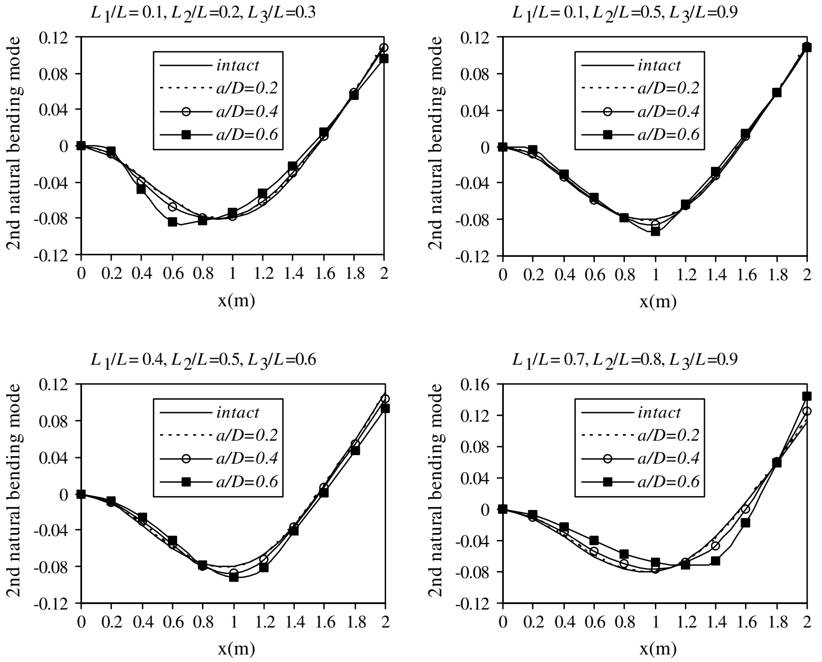

Fig. 8. Second natural bending mode as a function of various crack depth ratios ($a/D = 0.2$, $a/D = 0.4$, $a/D = 0.6$) for several crack locations ($L_1/L = 0.1$, $L_2/L = 0.2$, $L_3/L = 0.3$), ($L_1/L = 0.1$, $L_2/L = 0.5$, $L_3/L = 0.9$), ($L_1/L = 0.4$, $L_2/L = 0.5$, $L_3/L = 0.6$) and ($L_1/L = 0.7$, $L_2/L = 0.8$, $L_3/L = 0.9$).

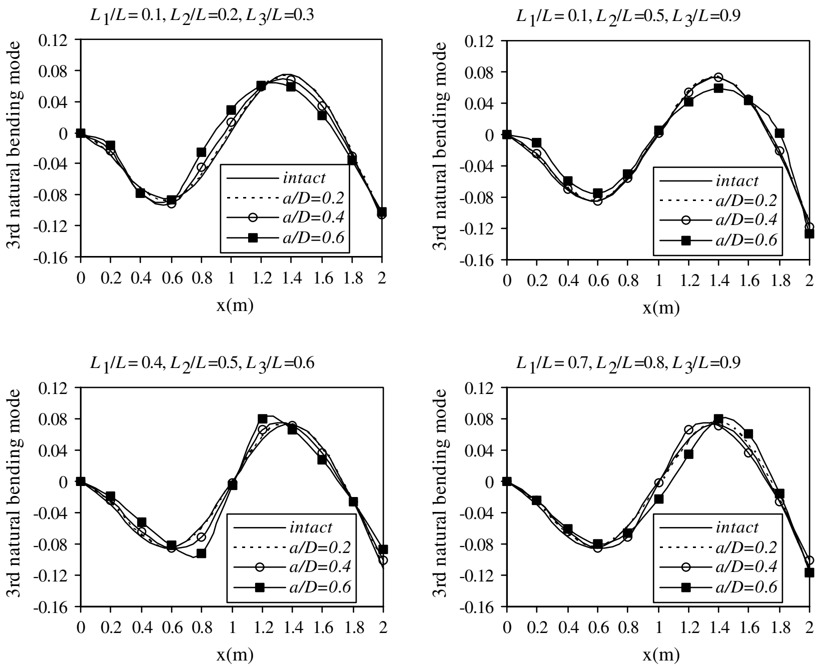

Fig. 9. Third natural bending mode as a function of various crack depth ratios ($a/D = 0.2$, $a/D = 0.4$, $a/D = 0.6$) for several crack locations ($L_1/L = 0.1$, $L_2/L = 0.2$, $L_3/L = 0.3$), ($L_1/L = 0.1$, $L_2/L = 0.5$, $L_3/L = 0.9$), ($L_1/L = 0.4$, $L_2/L = 0.5$, $L_3/L = 0.6$) and ($L_1/L = 0.7$, $L_2/L = 0.8$, $L_3/L = 0.9$).

3.3. Simply supported beam with multiple cracks

Third example is chosen as a simply supported beam having three cracks of equal depths as shown in Fig. 10. Again, the material and geometrical properties of the beam are identical to those of previous cases. Fig. 11 presents the first, second and third non-dimensional natural frequencies as a function of crack depth ratio for several crack locations ($L_1/L = 0.1$, $L_2/L = 0.2$, $L_3/L = 0.3$), ($L_1/L = 0.1$, $L_2/L = 0.5$, $L_3/L = 0.9$), ($L_1/L = 0.4$, $L_2/L = 0.5$, $L_3/L = 0.6$) and ($L_1/L = 0.7$, $L_2/L = 0.8$, $L_3/L = 0.9$).

Consider two cases in which the cracks are located at $L_1/L = 0.1$, $L_2/L = 0.2$, $L_3/L = 0.3$ and $L_1/L = 0.7$, $L_2/L = 0.8$, $L_3/L = 0.9$, respectively. As geometry of the beam and aforementioned two cases are symmetric, the changes in the natural frequencies are the same, Fig. 11. If the cracks are located near the support points ($L_1/L = 0.1$, $L_2/L = 0.2$, $L_3/L = 0.3$) or ($L_1/L = 0.7$, $L_2/L = 0.8$, $L_3/L = 0.9$) then the reduction in the second and third natural frequencies is higher. Conversely, the greater drops in the first natural frequency are observed when the cracks are located close to the midpoint of the beam ($L_1/L = 0.4$, $L_2/L = 0.5$, $L_3/L = 0.6$). This is for the reason that the crack positions are at the site where the first mode bending moment, which dominates the behaviour of the cracked beam, is highest.

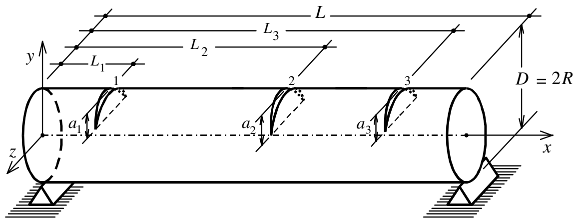

Fig. 10. Geometry of the simply supported circular beam with multiple cracks.

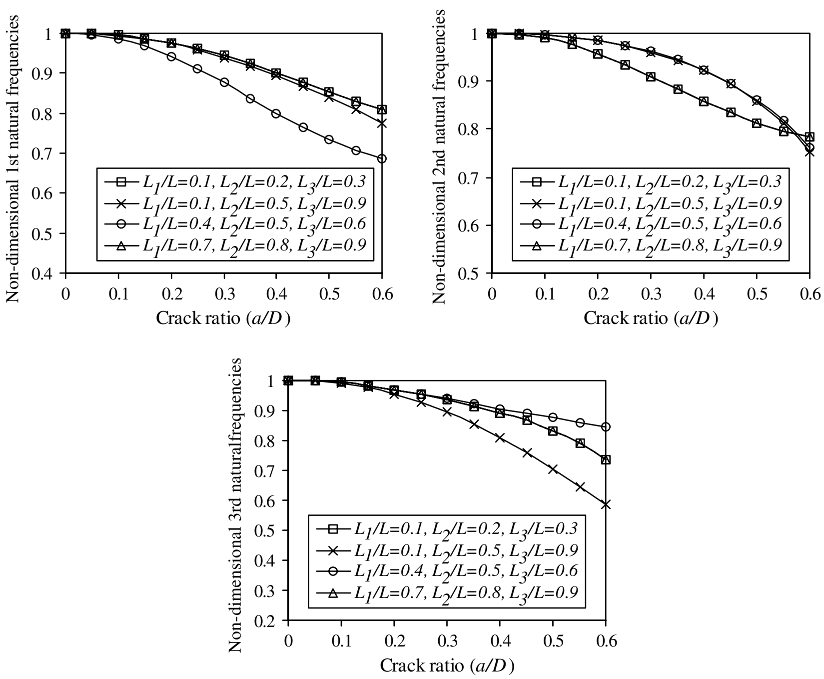

Fig. 11. First, second and third non-dimensional natural frequencies as a function of crack depth ratio for several crack locations ($L_1/L = 0.1$, $L_2/L = 0.2$, $L_3/L = 0.3$), ($L_1/L = 0.1$, $L_2/L = 0.5$, $L_3/L = 0.9$), ($L_1/L = 0.4$, $L_2/L = 0.5$, $L_3/L = 0.6$) and ($L_1/L = 0.7$, $L_2/L = 0.8$, $L_3/L = 0.9$).

Figs. 12–14 illustrate the first, second and third natural bending mode shapes as a function of crack depth ratios for various crack locations. It is clear from the mode shapes that the position of the cracks can be

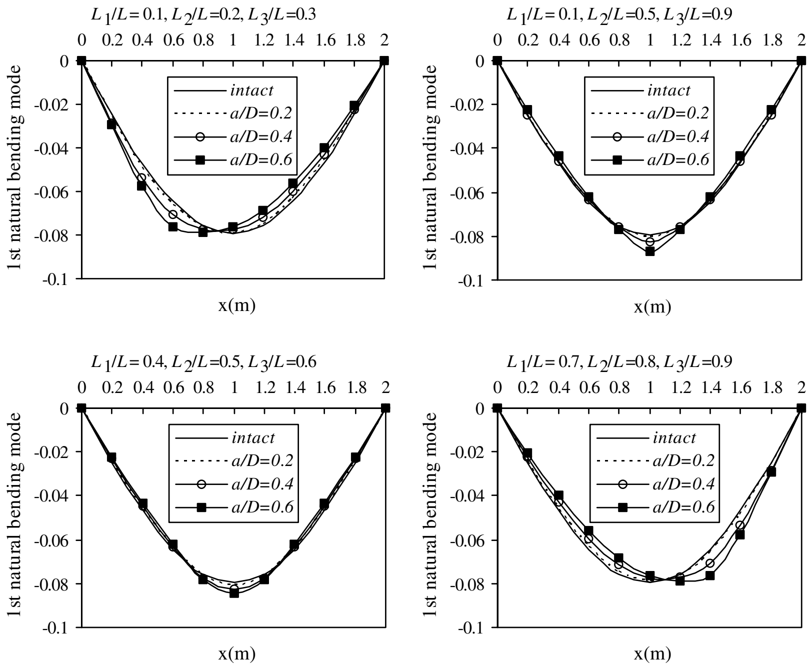

Fig. 12. First natural bending mode as a function of various crack depth ratios ($a/D = 0.2$, $a/D = 0.4$, $a/D = 0.6$) for several crack locations ($L_1/L = 0.1$, $L_2/L = 0.2$, $L_3/L = 0.3$), ($L_1/L = 0.1$, $L_2/L = 0.5$, $L_3/L = 0.9$), ($L_1/L = 0.4$, $L_2/L = 0.5$, $L_3/L = 0.6$) and ($L_1/L = 0.7$, $L_2/L = 0.8$, $L_3/L = 0.9$).

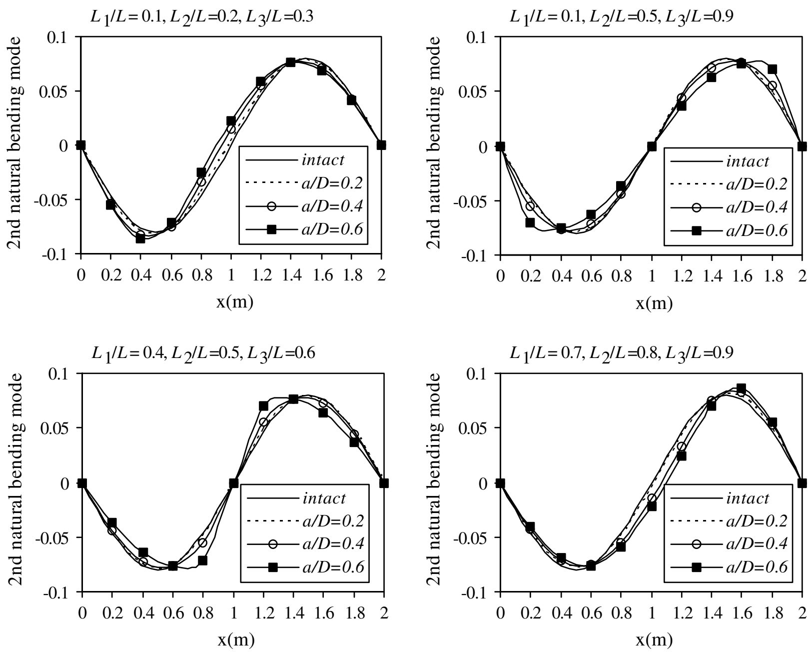

Fig. 13. Second natural bending mode as a function of various crack depth ratios ($a/D = 0.2$, $a/D = 0.4$, $a/D = 0.6$) for several crack locations ($L_1/L = 0.1$, $L_2/L = 0.2$, $L_3/L = 0.3$), ($L_1/L = 0.1$, $L_2/L = 0.5$, $L_3/L = 0.9$), ($L_1/L = 0.4$, $L_2/L = 0.5$, $L_3/L = 0.6$) and ($L_1/L = 0.7$, $L_2/L = 0.8$, $L_3/L = 0.9$).

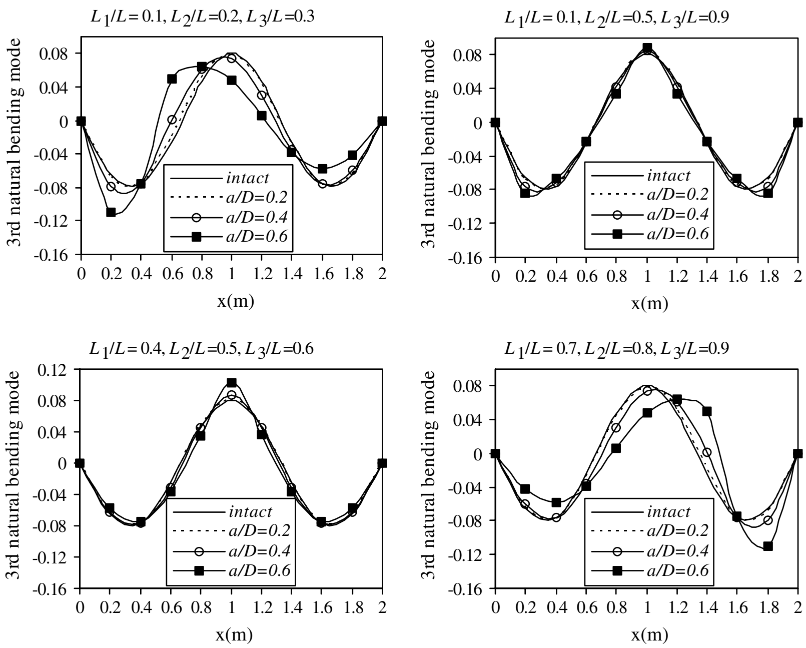

Fig. 14. Third natural bending mode as a function of various crack depth ratios ($a/D = 0.2$, $a/D = 0.4$, $a/D = 0.6$) for several crack locations ($L_1/L = 0.1$, $L_2/L = 0.2$, $L_3/L = 0.3$), ($L_1/L = 0.1$, $L_2/L = 0.5$, $L_3/L = 0.9$), ($L_1/L = 0.4$, $L_2/L = 0.5$, $L_3/L = 0.6$) and ($L_1/L = 0.7$, $L_2/L = 0.8$, $L_3/L = 0.9$).

evidently determined, as a consequence it can be concluded that mode shapes give useful information especially about the position of cracks.

4. Conclusions

In this paper, a new numerical approach to implement the free vibration analysis of circular cross sectional beams containing multiple non-propagating open cracks is presented. In the approach the component mode synthesis technique is combined with the finite element method and a non-linear problem separated into linear subsystems. The validation of the proposed method is carried out with three examples and it is shown that the modal characteristics, i.e. natural frequencies and mode shapes of a beam are depend on the location and depth of cracks. Moreover, it is revealed that the modal data provides useful information for the determination of structural defects such as cracks.

As the whole structure is detached from the crack sections, the present model enables also one to investigate the non-linear interface effects such as contact and impact when the cracks breathe. Although the analysis of the present study is mainly for beams with constant cross sections, extension to tapered beams can be carried out easily. Other possible extensions of the study are the inclusion of damping effects, as well as the propagation of cracks, which are left for future works.

References

[1] Cawley P, Adams RD. The location of defects in structures from measurements of natural frequencies. J Strain Anal 1979;14:49–57.
[2] Gounaris G, Dimarogonas AD. A finite element of a cracked prismatic beam for structural analysis. Comput Struct 1988;28:309–13.
[3] Shen MHH, Chu YC. Vibrations of beams with a fatigue crack. Comput Struct 1992;45:79–93.
[4] Krawczuk M, Ostachowicz WM. Transverse natural vibrations of a cracked beam loaded with a constant axial force. J Vib Acoust 1993;115:524–8.
[5] Ruotolo R, Surace C, Crespo P, Storer D. Harmonic analysis of the vibrations of a cantilevered beam with a closing crack. Comput Struct 1996;61:1057–74.

[6] Kisa M, Brandon JA, Topcu M. Free vibration analysis of cracked beams by a combination of finite elements and component mode synthesis methods. Comput Struct 1998;67:215–23.
[7] Shifrin EI, Ruotolo R. Natural frequencies of a beam with an arbitrary number of cracks. J Sound Vib 1999;223:409–23.
[8] Kisa M, Brandon JA. Free vibration analysis of multiple open-edge cracked beams by component mode synthesis. Struct Eng Mech 2000;10:81–92.
[9] Kisa M, Brandon JA. The effects of closure of cracks on the dynamics of a cracked cantilever beam. J Sound Vib 2000;238:1–18.
[10] Viola E, Federici L, Nobie L. Detection of crack location using cracked beam element method for structural analysis. Theor Appl Fract Mech 2001;36:23–35.
[11] Krawczuk M. Application of spectral beam finite element with a crack and iterative search technique for damage detection. Finite Elem Anal Des 2002;38:537–48.
[12] Patil DP, Maiti SK. Detection of multiple cracks using frequency measurements. Eng Fract Mech 2003;70:553–72.
[13] Kisa M. Free vibration analysis of a cantilever composite beam with multiple cracks. Compos Sci Technol 2004;64:1391–402.
[14] Gudmundson P. The dynamic behaviour of slender structures with cross-sectional cracks. J Mech Phys Solids 1983;31:329–45.
[15] Yuen MMF. A numerical study of the eigenparameters of a damaged cantilever. J Sound Vib 1985;103:301–10.
[16] Qian GL, Gu SN, Jiang JS. The dynamic behaviour and crack detection of a beam with a crack. J Sound Vib 1990;138:233–43.
[17] Rizos PF, Aspragathos N, Dimarogonas AD. Identification of crack location and magnitude in a cantilever beam from the vibration modes. J Sound Vib 1990;138:381–8.
[18] Shen MHH, Taylor JE. An identification problem for vibrating cracked beams. J Sound Vib 1991;150:457–84.
[19] Dimarogonas AD, Papadopoulos CA. Vibrations of cracked shafts in bending. J Sound Vib 1983;91:583–93.
[20] Papadopoulos CA, Dimarogonas AD. Coupled longitudinal and bending vibrations of a rotating shaft with an open crack. J Sound Vib 1987;117:81–93.
[21] Kikidis ML, Papadopoulos CA. Slenderness ratio effect on cracked beam. J Sound Vib 1992;155:1–11.
[22] Zheng DY, Fan SC. Vibration and stability of cracked hollow-sectional beams. J Sound Vib 2003;267:933–54.
[23] Dong GM, Chen J, Zou J. Parameter identification of a rotor with an open crack. Eur J Mech A/Solids 2004;23:325–33.
[24] Tsai TC, Wang YZ. The vibration of a multi-crack rotor. Int J Mech Sci 1997;39:1037–53.
[25] Darpe AK, Gupta K, Chawla A. Dynamics of a two-crack rotor. J Sound Vib 2003;259:649–75.
[26] Sekhar AS. Vibration characteristics of a cracked rotor with two open cracks. J Sound Vib 1999;223:497–512.
[27] Sekhar AS. Model-based identification of two cracks in a rotor system. Mech Syst Signal Process 2004;18:977–83.
[28] Ruotolo R, Surace C. Damage assessment of multiple cracked beams: numerical results and experimental validation. J Sound Vib 1997;206:567–88.
[29] Zheng DY, Fan SC. Natural frequencies of a non-uniform beam with multiple cracks via modified Fourier series. J Sound Vib 2001;242:701–17.
[30] Li QS. Vibratory characteristics of multi-step beams with an arbitrary number of cracks and concentrated masses. Appl Acoust 2001;62:691–706.
[31] Li QS. Free vibration analysis of non-uniform beams with an arbitrary number of cracks and concentrated masses. J Sound Vib 2001;252:509–25.
[32] Khiem NT, Lien TV. A simplified method for natural frequency analysis of a multiple cracked beam. J Sound Vib 2001;245:737–51.
[33] Lin HP, Chang SC, Wu JD. Beam vibrations with an arbitrary number of cracks. J Sound Vib 2002;258:987–99.
[34] Ruotolo R, Surace C. Natural frequencies of a bar with multiple cracks. J Sound Vib 2004;272:301–16.
[35] Patil DP, Maiti SK. Experimental verification of a method of detection of multiple cracks in beams based on frequency measurements. J Sound Vib 2005;281:439–51.
[36] Chang CC, Chen LW. Detection of the location and size of cracks in the multiple cracked beam by spatial wavelet based approach. Mech Syst Signal Process 2005;19:139–55.
[37] Binici B. Vibration of beams with multiple open cracks subjected to axial force. J Sound Vib 2005;287:277–95.
[38] Abraham ONL, Brandon JA. The modelling of the opening and closure of a crack. J Vib Acoust 1995;117:370–7.
[39] Brandon JA, Abraham ONL. Counter-intuitive quasi-periodic motion in the autonomous vibration of cracked Timoshenko beams. J Sound Vib 1995;185:415–30.
[40] Hurty WC. Dynamic analysis of structures using substructure modes. AIAA J 1965;3:678–85.
[41] Irwin G. Fracture mechanics, structural mechanics. Pergamon Press; 1960.
[42] Dimarogonas AD, Paipetis SA. Analytical methods in rotor dynamics. Applied Science Publishers; 1983.
[43] Friedman Z, Kosmatka JB. An improved two-node Timoshenko beam finite element. Comput Struct 1993;47:473–81.
[44] Papadopoulos CA, Dimarogonas AD. Coupled longitudinal and bending vibrations of a cracked shaft. J Vibr Acoust Stress Rel Des 1988;110:1–8.